

Seismic performance of mid-rise steel frames with semi-rigid connections having different moment capacity

Mohammad Bayat^{1a} and Seyed Mehdi Zahrai^{*2}

¹ School of Civil Engineering, the University of Tehran, Iran

² Center of Excellence for Engineering and Management of Civil Infrastructures, School of Civil Engineering, The University of Tehran, P.O. Box 11155-4563, Tehran, Iran

(Received March 02, 2017, Revised May 01, 2017, Accepted May 19, 2017)

Abstract. Seismic performance of hybrid steel frames defined as mixture of rigid and semi-rigid connections is investigated in this paper. Three frames with 10, 15 and 20 stories are designed with fully rigid connections and then with 4 patterns for semi-rigid connection placement, some of beam to column rigid connections would turn to semi-rigid. Each semi-rigid connection is considered with 4 different moment capacities and all rigid and semi-rigid frames consisting of 51 models are subjected to 5 selected earthquake records for nonlinear analysis. Maximum story drifts, roof acceleration and base shear are extracted for those 5 earthquake records and average values are obtained for each case. Based on numerical results for the proposed hybrid frames, story drifts remain in allowable range and the reductions in the maximum roof acceleration of 22, 29 and 25% and maximum base shear of 33, 31 and 54% occur in those 10, 15 and 20-story frames, respectively.

Keywords: semi-rigid connection; hybrid steel frame; seismic performance; moment capacity ratio

1. Introduction

After unexpected damage to fully welded connections in the Northridge and Kobe earthquakes several alternatives were investigated. One of the solutions was to use semi-rigid bolted connections instead of fully rigid connections. Several researchers investigated the ductility and energy dissipation capacity of semi-rigid connections. Experimental results showed that semi-rigid bolted connections have good ductility and can dissipate large amount of energy without failing. Researchers discovered the problem of old fully welded connections and they modified them to tolerate large rotations without fracture but because of ductility and good energy dissipating capacity, further studies continued on semi-rigid connections.

There are 4 connections known as semi-rigid including extended end plate, top and seat T-stub, end plate and top and seat angle. Ghobarah *et al.* (1990) have conducted 5 experiments on extended end plate connection to investigate the effect of design parameters on semi-rigid cyclic behavior. They found out that semi-rigid connections show high ductility with proper design. Latour and Rizzano (2012) discovered that top and seat T-stub will show high ductility by using hourglass shape for T shape parts web. Shi *et al.* (2007) conducted 8 experiments to investigate the effect of plate thickness, bolt size and column hardener on end plate connections behavior. Their results showed that

end plate connections have sufficient ductility and energy dissipation capacity for use in moment frames in seismic zones. Garlock *et al.* (2003) conducted an experiment on top and seat angle connections. They showed that this connection can dissipate large amount of energy even after formation of first yield point.

There are 4 ways to study on semi-rigid connections behavior including experimental, component, mathematical and Finite Element Method (FEM). In experimental method, connection is made in lab and is loaded by monotonic or cyclic load. Abidelah *et al.* (2012) conducted 8 experiments to investigate the effect of stiffeners on extended end plate connection behavior. Results showed that ultimate moment capacity and initial stiffness will increase but ductility will decrease by using stiffeners in such connections. In component method, a mechanical model of connection is made and any part of connection is modeled by a spring. Moment rotation curve is obtained by loading the model step by step and applying force and moment balance in model. Kim *et al.* (2010) modeled top and seat angle connection with component method. Their results showed that this model can predict behavior of connection properly. In FEM, connection is divided to finite elements and connections stiffness matrix is obtained by combining the stiffness matrix of this elements. Díaz *et al.* (2011) modeled end plate connection with FEM and their results showed that this method can predict the behavior of connection properly. In mathematical method, a formula is used with some coefficients for predicting the connections moment rotation curve. Frye and Morris (1975) used a 5-degree polynomial function with 3 coefficients and a standard parameter depending on connection geometry for predicting connection moment rotation curve.

*Corresponding author, Professor,
E-mail: mzahrai@ut.ac.it

^a M.Sc. Student

There are 3 ways for investigating semi-rigid frames including experimental method, rotational spring and hybrid model. In experimental method the frame should be built in lab and monotonic or cyclic load should be applied to it. Nader and Astanteh (1991) conducted an experiment on one bay one story to investigate behavior of semi-rigid frames and demonstrated that base shear will increase with connection stiffness increasing but lateral drift doesn't decrease the same. In rotational spring method the semi-rigid connections are modeled by a rotational spring. Moment rotation curve of semi-rigid connection is simplified with a multilinear curve. Kim and Choi (2001) modeled a one bay two story frame with semi-rigid connection using rotational spring for semi-rigid connections modeling. Comparison with experimental results showed that this method can predict the behavior of semi-rigid frames with high accuracy. In hybrid method, beams and columns are modeled with simple linear elements but connections are modeled in full detail. Sagiroglu and Aydin (2015) used rotation spring method for analyzing space semi-rigid frames. They used Frye-Morris method to model semi-rigid connection behavior and showed that this method can be used effectively for analyzing and designing of semi-rigid frames.

Mahmoud *et al.* (2013) modeled a two-story two-bay semi-rigid frame with hybrid method. Their results showed that this method can predict the behavior of frame accurately. They discovered that by semi-rigid connections capacity decreasing acceleration will decrease and connection will experience higher rotations. Rafiee *et al.* (2013) used big Bang-crunch algorithm for optimizing weight of frames by 8 different semi-rigid connections considering Frye-Morris model as their behavior curve. They showed that this method can be used for optimizing frame weight effectively through which connection type is very important.

Using hybrid frames (rigid and semi-rigid connections together) has been investigated by several researchers. Kishi *et al.* (1996) modeled a four-bay eight-story frame with combination of rigid and semi-rigid connections. They discovered that with proper pattern for semi-rigid connections location one can decrease base shear and keep drifts in allowable range. Akbas and Shen (2003) modeled 5 and 10-story frames in hybrid manner and showed that base shear will decrease in such frames compared to fully rigid frames. Razavi and Abolmaali (2014) investigated the effect of using combination of rigid and semi-rigid connections for a 20-story frame. They used 5 patterns for semi-rigid connections location. Patterns were including middle stories in all bays, above stories middle bays, above stories one middle bay, all stories one middle bay and all stories zigzag pattern for bay. Their results showed that zigzag pattern had the least drifts even less than rigid frame. In this pattern, beams and columns moment and shear decreased by 6 to 16 percent compared to rigid frame. Feizi *et al.* (2015) modeled 3 frames with 3, 8 and 15 stories as rigid, semi-rigid and hybrid frames and demonstrated that among all studied frames there is a hybrid frame that has better seismic performance than rigid frame based on base shear and story drifts.

Several studies have focused on semi-rigid connections

and their frames. Researchers have shown that semi-rigid connections have stable behavior and high ductility that can dissipate large amount of energy. However, using hybrid frames, i.e., combination of rigid and semi-rigid connections together, has been paid attention by just few researchers. This paper focuses on the best pattern for locations of semi-rigid connections among several proposed patterns and investigates the effect of number of stories and connection capacity on the seismic behavior of semi-rigid frames leading to the best possible pattern. Connection capacity percent in this research means the ratio of connection strength capacity to the strength capacity of the beam.

2. Method of study

The main objective of this study is to compare seismic performances of mid-rise steel rigid and hybrid frames (defined as a frame with mixture of rigid and semi-rigid connections). For this purpose, 3 rigid frames with 10, 15 and 20 stories are designed. Height to width ratios for these frames are 1.75, 2.62 and 3.5. ETABS software is used for modeling, design and nonlinear analyzing of all rigid and semi-rigid frames. All rigid frames are designed based on AISC360 criteria. To start, proper sections are assigned to the beams and columns. Dead and live loads are applied as linear loads on beams. Static equivalent method is used for considering seismic loads effect by applying base shear coefficient calculated based on ASCE 7. Internal forces obtained from the analysis are used to design each beam and column. Changing sections would cause change in

Table 1 Beam and column sections at different stories

Number of stories	stories	Beam sections	Column sections
10	1	B320-160-20-10	C350-350-24-10
	2-5	B350-180-20-10	C350-350-24-10
	6	B320-160-20-10	C350-350-24-10
	7	B320-160-20-10	C300-300-24-10
	8	B280-130-20-10	C300-300-24-10
	9,10	B280-130-20-10	C260-260-20-8
15	1-8	B350-200-24-12	C400-400-30-14
	9	B350-200-24-12	C350-350-26-12
	10-12	B320-160-22-12	C350-350-26-12
	13-15	B280-130-20-10	C300-300-24-10
20	1	B320-160-22-12	C450-450-30-14
	2-5	B350-200-24-12	C450-450-30-14
	6-9	B350-200-24-12	C400-400-30-14
	10	B320-160-22-12	C400-400-30-14
	11	B350-200-24-12	C400-400-30-14
	12-14	B320-160-22-12	C400-400-30-14
	15	B280-130-20-10	C400-400-30-14
	16	B320-160-22-12	C300-300-24-12
17-20	B280-130-20-10	C300-300-24-12	

internal forces so new analysis is needed. Thus, new internal forces are used for redesigning the beams and columns. All beams and columns are designed by repeating this trend until designed sections are recognized acceptable. Table 1 presents designed sections of beams and columns for 3 rigid frames.

In order to compare rigid and hybrid frames seismic performance, the same designed sections for rigid and hybrid frames are used. In this research, semi-rigid connection locations in hybrid frames are based on 4 different patterns including diagonal, double diagonal, middle and middle diagonal shown in Figs. 1-4. Rigid connections are modeled based on FEMA356. Nonlinear behavior model used for semi-rigid connections is based on experimental data suggested by authors as shown in Fig. 5. Nonlinear link element and hinge are used for modeling behavior of the semi-rigid and rigid connections. All frames are subjected to 5 earthquake record presented in Table 3. For each rigid frame, there are 16 hybrid frames because of

4 semi-rigid connection location patterns and 4 connection capacities leading to 51 total frames. Maximum story drifts, roof acceleration and base shear will be used for comparing seismic performance of rigid and hybrid frames. Acceptable maximum story drift is 2% for life safety performance level and 4% for collapse prevention performance level.

3. Numerical modeling

The frames are designed with self-defined girders. Table 1 presents used sections for 3 designed frames at different stories. Beam section names are expressed as $Bh-w-tf-tw$ where h , w , tf and tw represent respectively the height, the flange width, the flange thickness and the web thickness all in mm. Column section names are similar to beam section names except for C that stands for column.

As mentioned earlier, in this research, 3 frames with 10, 15 and 20 stories are used. All frames have 4 bays with 5

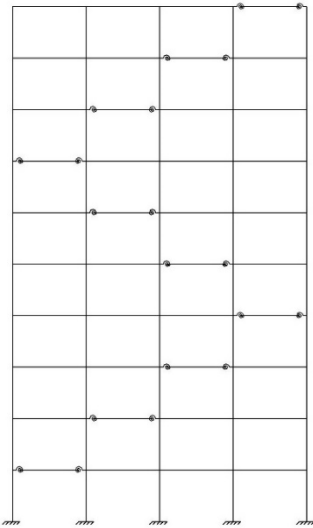


Fig. 1 Diagonal pattern for semi-rigid connection placement

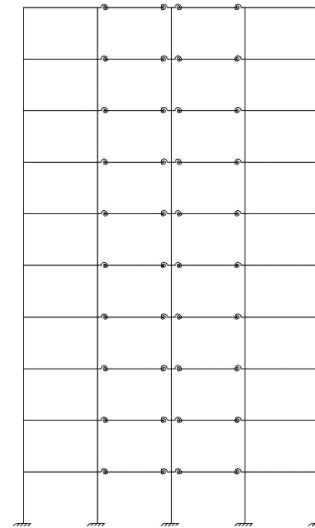


Fig. 3 Middle pattern for semi-rigid connection placement

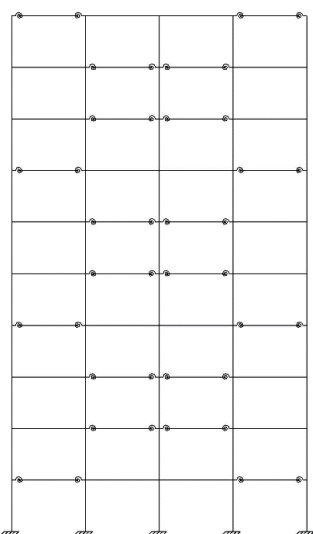


Fig. 2 Double diagonal pattern for semi-rigid connection placement

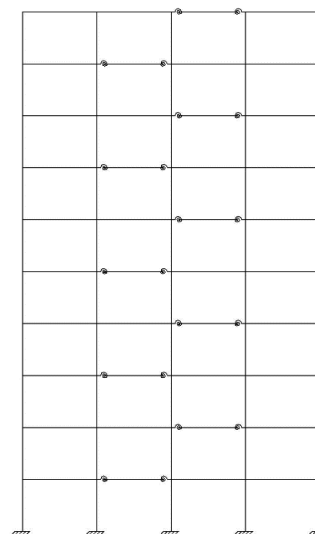


Fig. 4 Middle diagonal pattern for semi-rigid connection placement

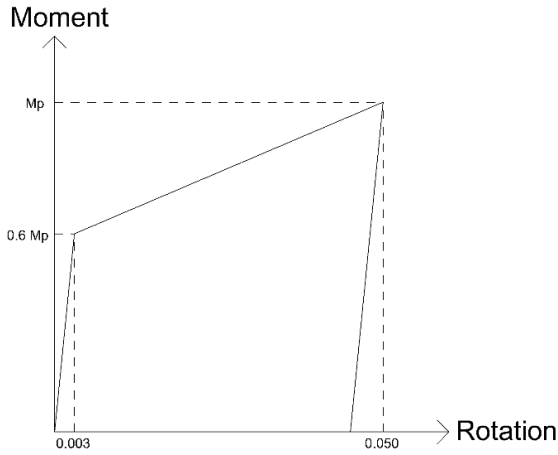


Fig. 5 Semi-rigid connection behavior

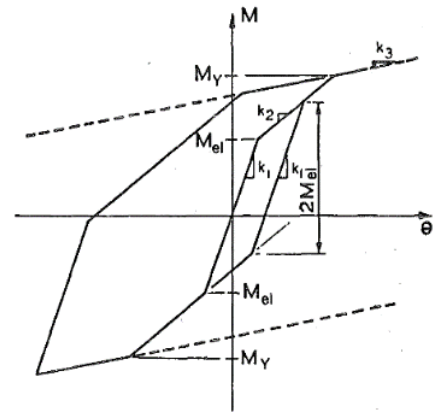


Fig. 7 Simplified behavior of semi-rigid connection (Stelmack *et al.* 1986)

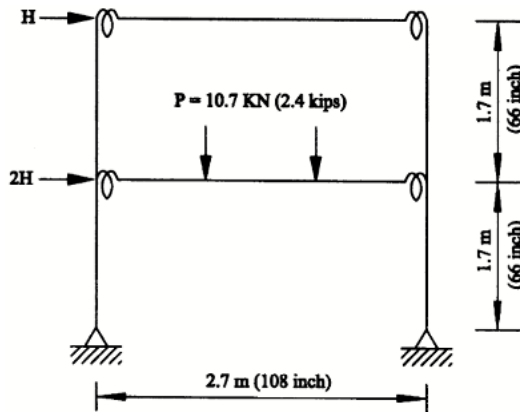


Fig. 6 Frame's geometry and loading (Stelmack *et al.* 1986)

meter span and 3.5 meter story height. Four patterns for semi-rigid connection placement including diagonal, double diagonal, middle and middle diagonal are considered as shown in Figs. 1 to 4.

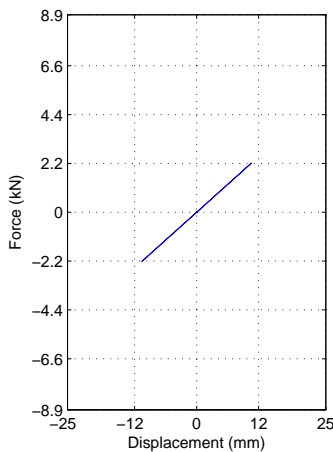
Rigid connections are modeled with Hinge according to FEMA 356 (its Tables 5-6). Two linear curves for semi-

rigid connection behavior modeling are used as shown in Fig. 5. Connection capacity ratios defined as connections plastic moment to beams plastic moment ratios are expressed in percent. Semi-rigid connections with 30, 45, 60 and 75% connection strength capacities are considered here.

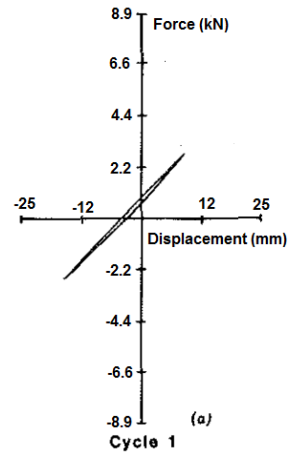
Rayleigh damping is used considering 5 percent damping for the 1st and 5th vibration modes of the frames. 5 kN/m² dead load and 2 kN/m² live load are assumed for the stories and 4 kN/m² dead load and 1.5 kN/m² live load for the roof. Also, FEMA356 load combination is used for nonlinear analysis. Frames are designed based on satisfying design criteria of AISC306 and assuming first vibration mode of frames linear. Girder sections are used for beams and columns.

4. Numerical model verification

Stelmack *et al.* (1986) has conducted an experiment on a one bay two-story semi-rigid frame. Frame geometry and loading shown in Fig. 6 simplified behavior of semi-rigid connection as shown in Fig. 7. Numerical and experimental results for force displacement curve of the first, second and



(a) Numerical results



(b) Experimental (Stelmack *et al.* 1986)

Fig. 8 Numerical and experimental results of the first loading cycle

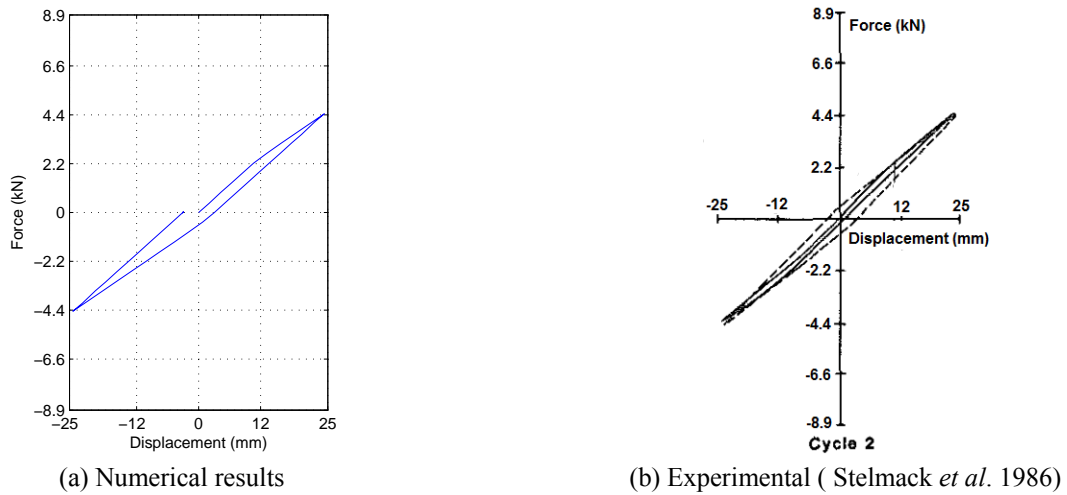


Fig. 9 Numerical and experimental results of the second loading cycle

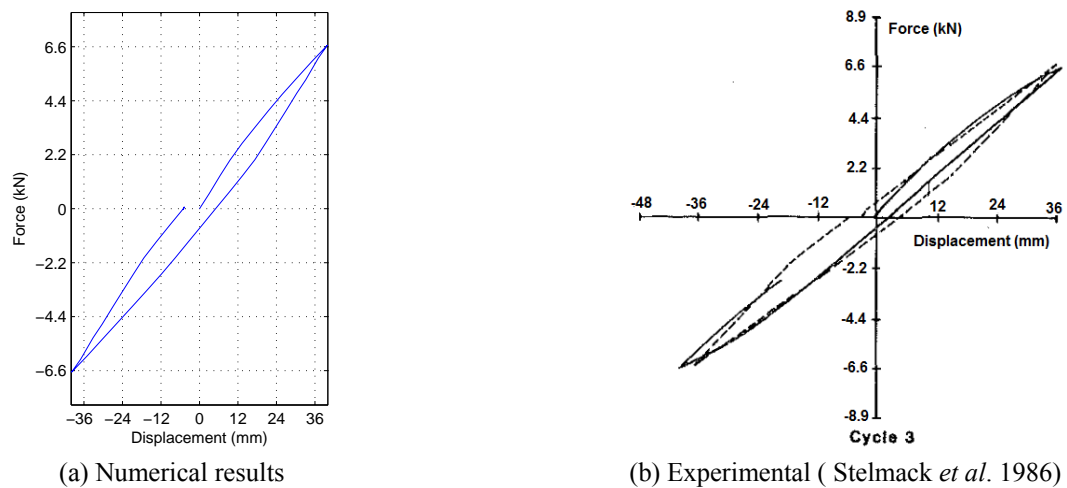


Fig. 10 Numerical and experimental results of third loading cycle

Table 2 Properties of earthquake records used for numerical analysis

Earthquake name	Intensity (Richter)	Distance to fault (km)	D5-75 (s)	D5-95 (s)
Bam	6.6	47	11.5	19.4
Chi-Chi	6.2	25	9.3	18.6
Imperial Valley	6.5	22	8.9	21.6
Kobe	6.9	21	8.2	13.2
Northridge	6.7	31	9.4	20.1

third loading cycle are shown in Figs. 8 to 10.

Properties of the earthquake records used for numerical analysis in this paper are presented in Table 2.

5. Numerical results

Table 3 presents main periods of all rigid and hybrid frames. As expected, main periods of the frames increase by story number and with increasing number of semi-rigid

connection and decreasing semi-rigid connection capacity.

Time history of roof displacement for connection with 60 percent capacity subjected to the Northridge record is shown in Figs. 11 to 15 where residual displacement in all frames is about 10 mm. Maximum roof displacements of semi-rigid frames are lower than those of the rigid frames but semi-rigid frames have more cycles with high maximum displacement.

Table 4 presents the maximum roof story displacement of 60% capacity semi-rigid frames and rigid frame subjected to 5 earthquake records.

Energy curves of rigid and semi-rigid frames with 60% capacity connections are shown in Figs. 16 to 20.

Semi-rigid frames have lower rigidity so they have higher period but all their main period is higher than 2 seconds so they have almost equal spectral acceleration value then as we discussed It can be concluded from Figs. 16 to 20 that maximum input energy of rigid frame is equal to those of semi-rigid frames but final value in rigid frame is lower than those of semi-rigid frames from 40 to 45%. It can also be concluded that nonlinear hysteresis damping in double diagonal and middle pattern is 32% higher than those of 2 other patterns.

Table 3 Main periods of analyzed framhpges

Number of stories	Connection capacity (%)	Location patterns for semi-rigid connections				Rigid (s)
		Diagonal (s)	Double diagonal (s)	Middle (s)	Middle diagonal (s)	
10	30	2.22	2.41	2.42	2.21	2.07
	45	2.19	2.34	2.34	2.19	
	60	2.17	2.29	2.29	2.17	
	75	2.16	2.26	2.26	2.16	
15	30	3.00	3.19	3.33	3.13	2.86
	45	2.97	3.13	3.20	3.03	
	60	2.94	3.09	3.12	2.97	
	75	2.93	3.06	3.06	2.92	
20	30	4.19	4.46	4.63	4.10	3.92
	45	4.13	4.24	4.43	4.04	
	60	4.08	4.10	4.30	3.99	
	75	4.05	3.98	4.21	3.96	

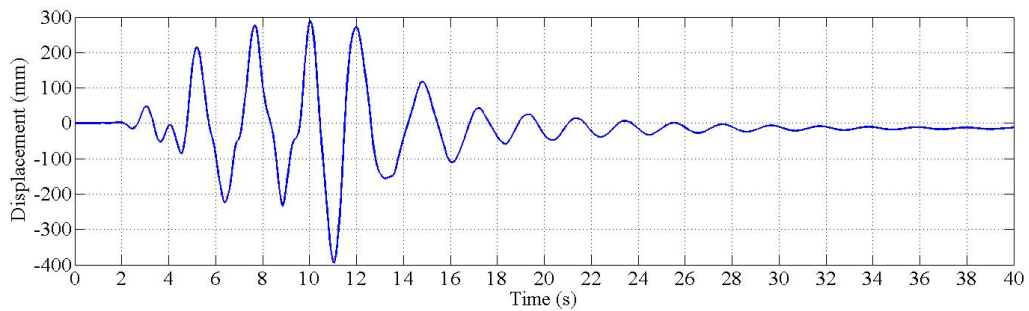


Fig. 11 Time history of roof displacement for 10-story rigid frame subjected to the Northridge record

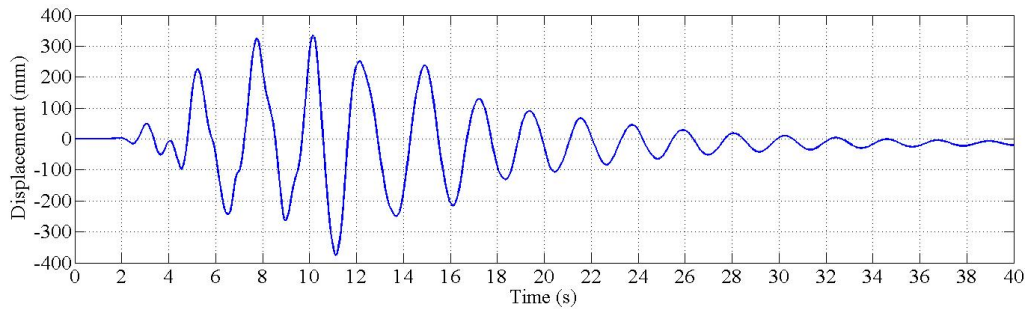


Fig. 12 Time history of roof displacement for 10-story frame with 60 percent capacity semi-rigid connections in diagonal pattern subjected to the Northridge record

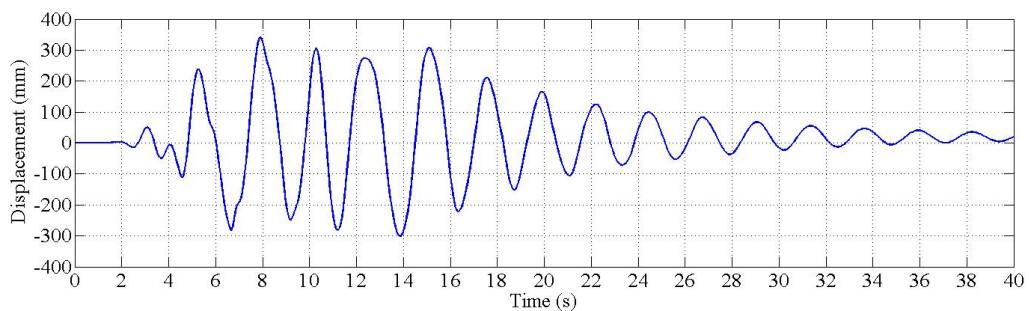


Fig. 13 Time history of roof displacement for 10 story frame with 60 percent capacity semi-rigid connections in double diagonal pattern subjected to the Northridge record

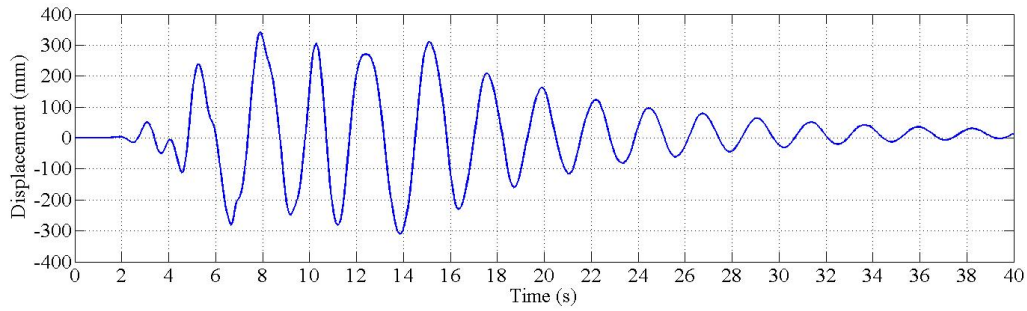


Fig. 14 Time history of roof displacement for 10-story frame with 60 percent capacity semi-rigid connections in middle pattern subjected to the Northridge record

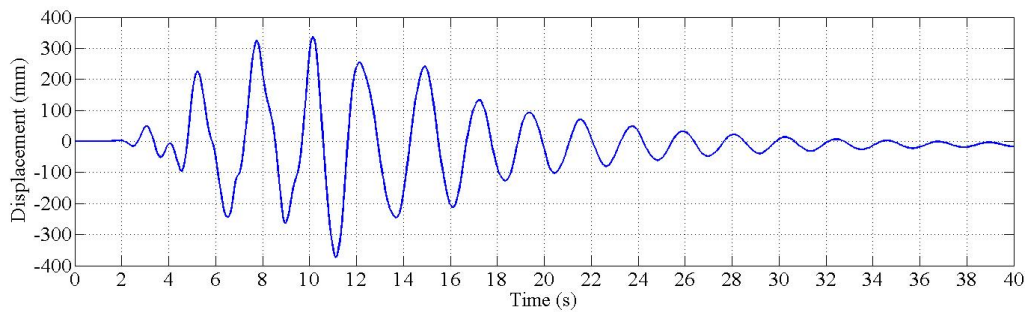


Fig. 15 Time history of roof displacement for 10-story frame with 60 percent capacity semi-rigid connections in middle diagonal pattern subjected to the Northridge record

Table 4 Maximum roof displacement of 60% capacity semi-rigid frames and rigid frames

Number of stories	Record name	Location patterns for semi rigid connections				Rigid frame (mm)
		Diagonal (mm)	Double diagonal (mm)	Middle (mm)	Middle diagonal (mm)	
10	Bam	357	408	412	357	401
	Chi-Chi	366	362	364	370	368
	Imperial	353	342	350	353	356
	Kobe	356	388	390	353	320
	Northridge	375	342	342	372	394
15	Bam	468	546	611	604	573
	Chi-Chi	509	535	525	575	572
	Imperial	482	461	538	567	568
	Kobe	448	458	574	579	544
	Northridge	665	578	560	533	712
20	Bam	724	529	522	751	702
	Chi-Chi	864	709	689	863	991
	Imperial	728	680	687	733	757
	Kobe	688	558	520	687	782
	Northridge	520	440	453	542	635

Hysteresis curves of semi-rigid connections for 10-story frame subjected to the Northridge record with diagonal pattern semi-rigid connections are shown in Figs. 21 to 24. The reason of choosing third floor for semi rigid connection hysteresis behavior curve is that the maximum story drift in this story is higher than other stories so nonlinear behavior of connection can be seen easier.

Connections with less capacity percent have less strength capacity so they yield sooner so experience more cycle and they have smaller moment value. It can be concluded from Figs. 21 to 24 that maximum rotation in all capacity ratios is almost equal to each other but maximum moment increase with increasing connection capacity. Number of cycles decrease with increasing connection capacity.

Maximum story drifts, roof acceleration and base shear of 4 semi-rigid connection placement patterns are shown in Figs. 25 to 27 for 10-story frame subjected to five selected earthquake records.

Tables 5-7 present the maximum story drift, roof accele-

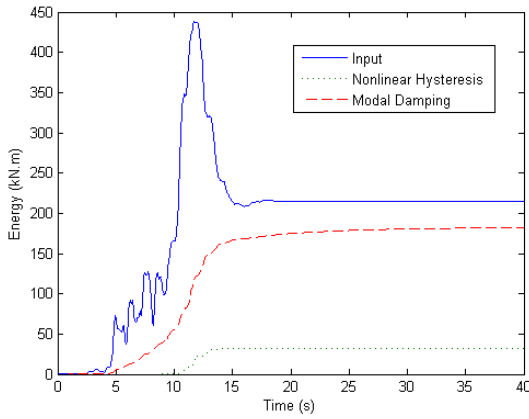


Fig. 16 Energy curve for 10-story rigid frame subjected to the Northridge record

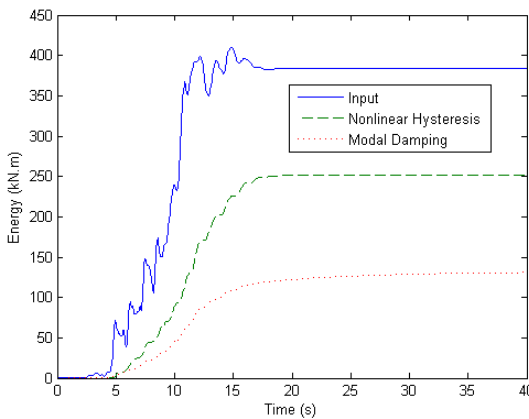


Fig. 17 Energy curve for 10-story frame with 60% capacity semi-rigid connections in diagonal pattern subjected to the Northridge record

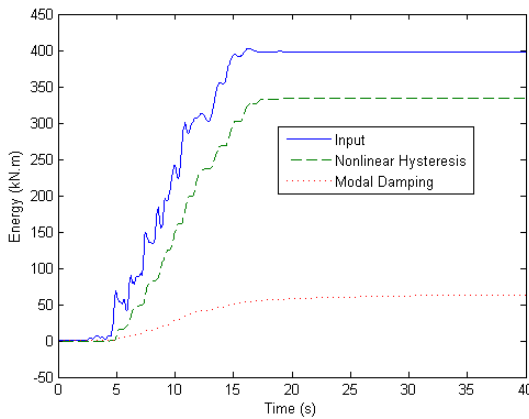


Fig. 18 Energy curve for 10-story frame with 60% capacity semi-rigid connections in double diagonal pattern subjected to the Northridge record

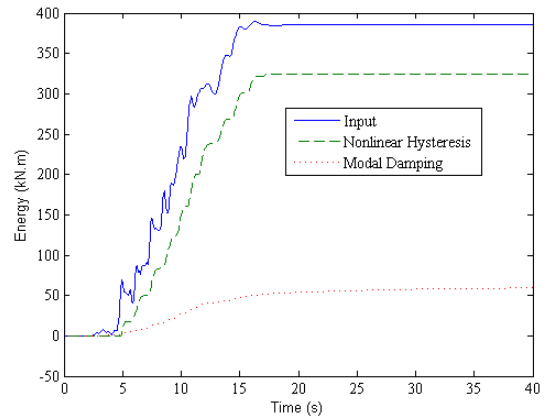


Fig. 19 Energy curve for 10-story frame with 60% capacity semi-rigid connections in middle pattern subjected to the Northridge record

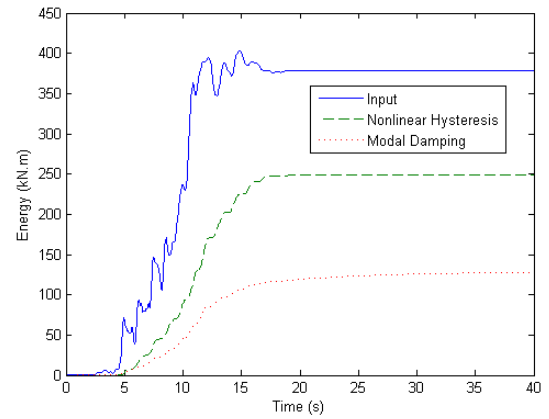


Fig. 20 Energy curve for 10-story frame with 60% capacity semi-rigid connections in middle diagonal pattern subjected to the Northridge record

ration and base shear of 10-story frames subjected to those 5 earthquake records.

Adding semi-rigid connections to a rigid frame has made 2 main effects: first, frame rigidity decrease specially

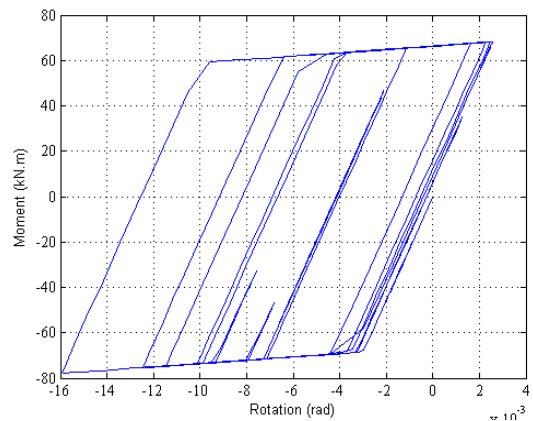


Fig. 21 Hysteresis behavior of third floor: semi-rigid connection with 30% capacity for diagonal pattern

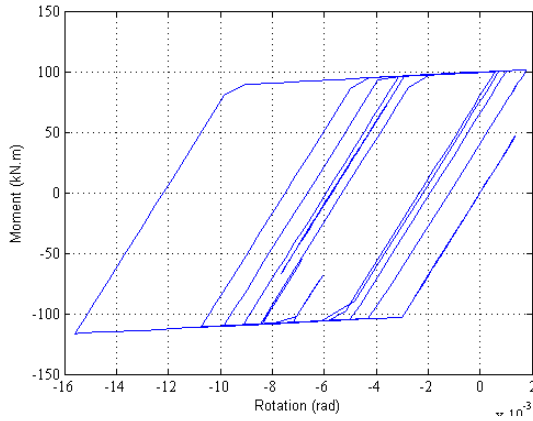


Fig. 22 Hysteresis behavior of third floor: semi-rigid connection with 45% capacity for diagonal pattern

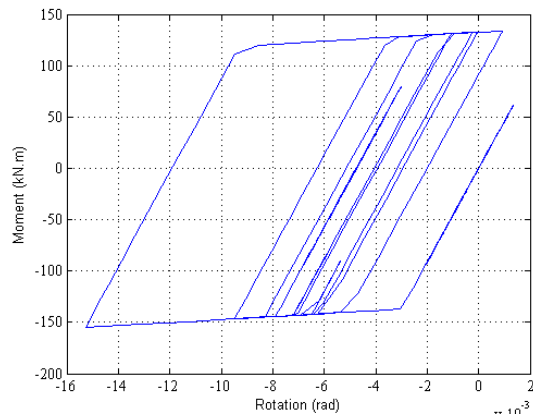


Fig. 23 Hysteresis behavior of third floor: semi-rigid connection with 60% capacity for diagonal pattern

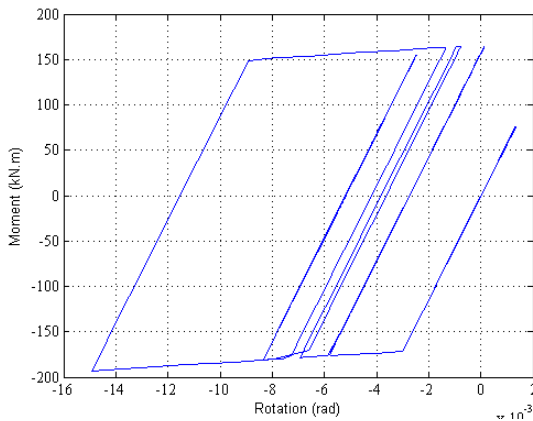


Fig. 24 Hysteresis behavior of third floor: semi-rigid connection with 75 percent capacity for diagonal pattern

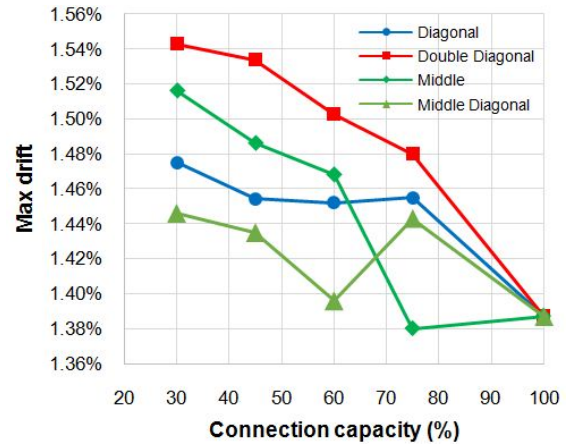


Fig. 25 Maximum story drifts of 10-story frame subjected to 5 earthquake records

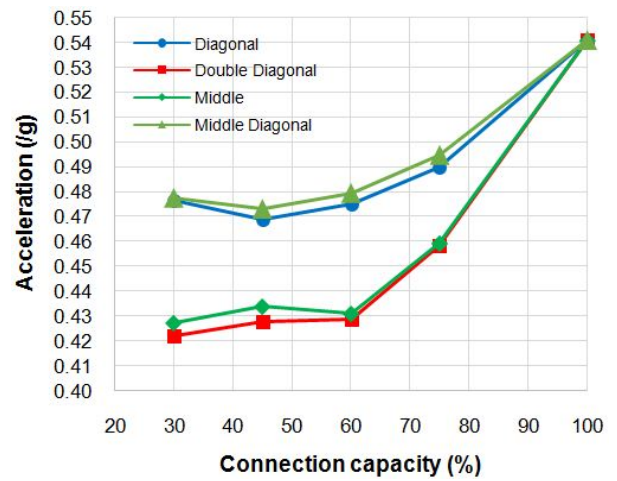


Fig. 26 Maximum roof acceleration of 10-story frame subjected to 5 earthquake records

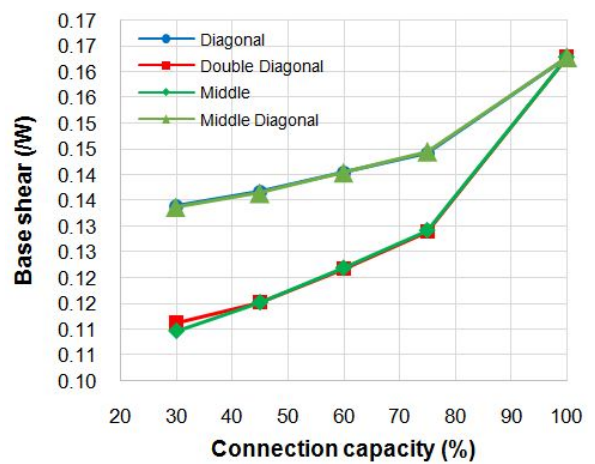


Fig. 27 Maximum base shear of 10-story frame subjected to 5 earthquake records

after yielding of semi-rigid connections; second, energy dissipation through semi-rigid connections that has made them like damper. Combination of these 2 main effects will cause decrease or increase of maximum story drifts. Results showed that in 10-story frames, rigidity decreasing has

higher effect so story drifts increased by using semi-rigid connections. For base shear and roof acceleration it is clear that by using semi rigid connection, rigidity of frame will decrease and the frame will behave more ductile so base

Table 5 Maximum story drift of 10-story frames

Record name	Connection capacity (%)	Location patterns for semi rigid connections				Rigid frame (%)
		Diagonal (%)	Double diagonal (%)	Middle (%)	Middle diagonal (%)	
Bam	30	1.42	1.55	1.51	1.39	1.48
	45	1.40	1.55	1.50	1.38	
	60	1.41	1.48	1.43	1.40	
	75	1.42	1.43	1.40	1.40	
Chi-Chi	30	1.25	1.70	1.61	1.22	1.17
	45	1.20	1.55	1.47	1.19	
	60	1.18	1.45	1.39	1.17	
	75	1.16	1.35	1.30	1.16	
Imperial	30	1.47	1.47	1.42	1.42	1.25
	45	1.42	1.44	1.40	1.39	
	60	1.39	1.45	1.42	1.35	
	75	1.39	1.48	1.44	1.38	
Kobe	30	1.65	1.47	1.50	1.63	1.32
	45	1.58	1.63	1.64	1.56	
	60	1.52	1.72	1.73	1.32	
	75	1.49	1.71	1.71	1.47	
Northridge	30	1.60	1.52	1.53	1.56	1.69
	45	1.67	1.50	1.42	1.65	
	60	1.75	1.41	1.38	1.74	
	75	1.83	1.43	1.05	1.81	

shear and roof acceleration will decrease too. According to Fig. 25, all semi-rigid frames have higher maximum drifts than rigid frame except for middle pattern at 75% capacity that is about 1% lower. Double diagonal pattern have the highest maximum drifts and middle diagonal have the least maximum drifts among semi-rigid frames. Using connection capacity that leads to a minimum value for maximum story drift, diagonal, double diagonal, middle and middle diagonal would have 5, 7, 1% lower and equal maximum drift compared to rigid frame. As observed in Fig. 26, all semi-rigid frames have less roof acceleration than rigid frame. Double diagonal have the least maximum roof acceleration and middle diagonal have the highest maximum roof acceleration among semi-rigid frames. By choosing the best connection capacity, roof acceleration can be reduced by 13, 22, 21 and 12 percent in diagonal, double diagonal, middle and middle diagonal patterns, respectively. Based on Fig. 27, double diagonal and middle pattern have the least maximum base shear while using the best connection capacity, one can reduce maximum base shear by 18% in diagonal and middle diagonal pattern and 32% in double diagonal and middle pattern.

Maximum story drifts, roof acceleration and base shear of 4 semi-rigid connection patterns are shown in Figs. 28 to 30 for 15-story frame. All values are average of maximum values for 5 earthquake records results of frames.

Tables 8-10 present the maximum story drift, roof acceleration and base shear of 15-story frames subjected to those 5 earthquake records.

In most 15-story frames energy dissipation of semi-rigid connections has higher effect than decreasing rigidity of frame so maximum story drift was decreased by using semi-rigid connection. Base shear and roof acceleration has decreased by connection capacity decreasing that is because of energy dissipating of semi rigid connections and frames rigidity decreasing. Based on Fig. 28, diagonal pattern with 30, 45 and 75% connection capacity and double diagonal pattern with 60% have the least maximum story drift. Optimum connection capacity for minimizing the maximum

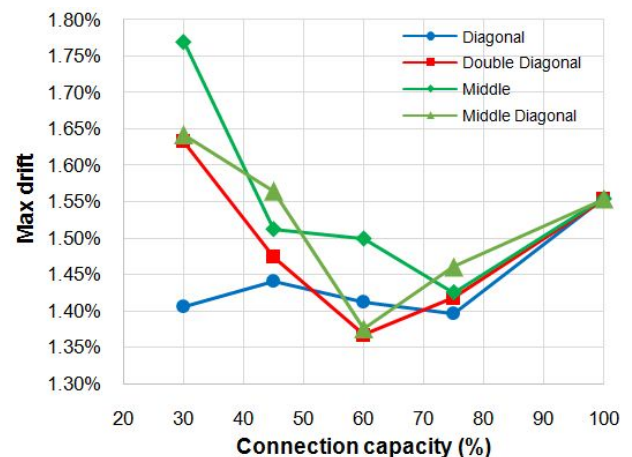


Fig. 28 Maximum story drifts of 15-story frame for different semi-rigid connection patterns

Table 6 Maximum roof acceleration of 10-story frames

Record name	Connection capacity (%)	Location patterns for semi rigid connections				Rigid frame (%)
		Diagonal (/g)	Double diagonal (/g)	Middle (/g)	Middle diagonal (/g)	
Bam	30	0.441	0.357	0.350	0.442	0.456
	45	0.431	0.393	0.394	0.426	
	60	0.425	0.429	0.427	0.420	
	75	0.418	0.448	0.442	0.417	
Chi-Chi	30	0.471	0.441	0.446	0.469	0.536
	45	0.473	0.446	0.444	0.476	
	60	0.479	0.450	0.443	0.480	
	75	0.479	0.455	0.453	0.483	
Imperial	30	0.426	0.368	0.364	0.427	0.554
	45	0.437	0.346	0.347	0.443	
	60	0.460	0.349	0.360	0.467	
	75	0.477	0.391	0.403	0.485	
Kobe	30	0.483	0.430	0.442	0.486	0.615
	45	0.468	0.456	0.471	0.468	
	60	0.480	0.465	0.465	0.492	
	75	0.508	0.498	0.503	0.518	
Northridge	30	0.561	0.514	0.534	0.564	0.544
	45	0.534	0.497	0.513	0.552	
	60	0.530	0.450	0.459	0.538	
	75	0.568	0.498	0.496	0.572	

Table 7 Maximum base shear of 10-story frames

Record name	Connection capacity (%)	Location patterns for semi rigid connections				Rigid frame (/W)
		Diagonal (/W)	Double diagonal (/W)	Middle (/W)	Middle diagonal (/W)	
Bam	30	0.135	0.117	0.118	0.136	0.156
	45	0.137	0.119	0.118	0.138	
	60	0.140	0.122	0.123	0.140	
	75	0.143	0.130	0.130	0.143	
Chi-Chi	30	0.128	0.109	0.106	0.127	0.156
	45	0.129	0.111	0.110	0.128	
	60	0.131	0.119	0.118	0.131	
	75	0.134	0.126	0.124	0.135	
Imperial	30	0.138	0.102	0.102	0.137	0.167
	45	0.142	0.112	0.113	0.142	
	60	0.146	0.122	0.122	0.147	
	75	0.150	0.130	0.130	0.151	
Kobe	30	0.139	0.119	0.117	0.139	0.162
	45	0.141	0.122	0.123	0.140	
	60	0.143	0.126	0.126	0.142	
	75	0.145	0.132	0.132	0.144	
Northridge	30	0.130	0.109	0.106	0.130	0.173
	45	0.134	0.113	0.112	0.135	
	60	0.143	0.121	0.120	0.143	
	75	0.150	0.127	0.129	0.150	

Table 8 Maximum story drift of 15-story frames

Record name	Connection capacity (%)	Location patterns for semi rigid connections				Rigid frame (W)
		Diagonal (%)	Double diagonal (%)	Middle (%)	Middle diagonal (%)	
Bam	30	1.74	1.88	1.69	1.79	1.59
	45	1.68	1.82	1.76	1.75	
	60	1.63	1.79	1.73	1.59	
	75	1.59	1.78	1.70	1.57	
Chi-Chi	30	1.36	1.45	2.14	1.50	1.70
	45	1.36	1.27	1.31	1.37	
	60	1.37	1.20	1.31	1.40	
	75	1.39	1.27	1.28	1.37	
Imperial	30	1.14	1.41	1.56	1.59	1.20
	45	1.16	1.23	1.33	1.47	
	60	1.18	1.15	1.33	1.28	
	75	1.19	1.13	1.21	1.15	
Kobe	30	1.44	1.75	1.44	1.51	1.71
	45	1.41	1.62	1.58	1.65	
	60	1.38	1.47	1.61	1.53	
	75	1.37	1.41	1.54	1.52	
Northridge	30	1.66	1.67	2.02	1.61	1.71
	45	1.60	1.44	1.57	1.48	
	60	1.52	1.23	1.50	1.48	
	75	1.44	1.50	1.39	1.44	

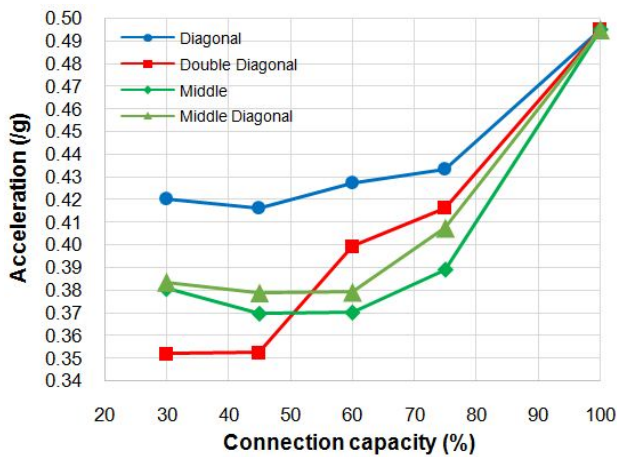


Fig. 29 Maximum roof acceleration of 15-story frame for different semi-rigid connection patterns

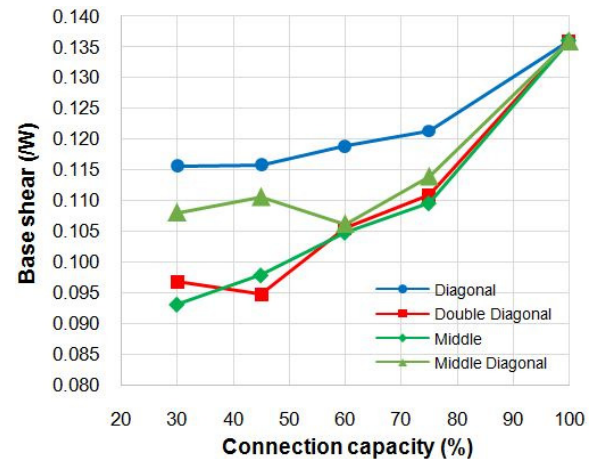


Fig. 30 Maximum base shear of 15-story frame for different semi-rigid connection patterns

story drift is between 60 and 75%. According to Fig. 29, double diagonal with connection capacity less than 50% and middle pattern with more than 50% connection capacity are the best patterns for roof acceleration. By choosing the best connection capacity one can reduce maximum roof acceleration by 16, 29, 25 and 23% in diagonal, double diagonal, middle and middle diagonal patterns. It is observed from Fig. 30 that middle pattern with 30, 60 and 75% connection capacity and double diagonal with 45% connection capacity have the least maximum base shears.

By using the best connection capacity, one can reduce maximum base shear by 15, 30, 31 and 22 percent in diagonal, double diagonal, middle and middle diagonal patterns.

Figs. 31 to 33 show Maximum story drifts, roof acceleration and base shear of 4 semi-rigid connection placement patterns for 20-story frame.

Tables 11-13 present the maximum story drift, roof acceleration and base shear of 20-story frames subjected to those 5 earthquake records.

Table 9 Maximum roof acceleration of 15-story frames

Record name	Connection capacity (%)	Location patterns for semi rigid connections				Rigid frame (/W)
		Diagonal (/g)	Double diagonal (/g)	Middle (/g)	Middle diagonal (/g)	
Bam	30	0.356	0.305	0.321	0.326	0.460
	45	0.348	0.298	0.307	0.315	
	60	0.387	0.342	0.327	0.322	
	75	0.401	0.368	0.346	0.360	
Chi-Chi	30	0.399	0.392	0.444	0.399	0.451
	45	0.411	0.338	0.454	0.377	
	60	0.403	0.385	0.408	0.350	
	75	0.406	0.394	0.369	0.388	
Imperial	30	0.419	0.386	0.402	0.420	0.458
	45	0.402	0.400	0.375	0.427	
	60	0.402	0.402	0.409	0.433	
	75	0.399	0.418	0.430	0.440	
Kobe	30	0.491	0.351	0.333	0.389	0.572
	45	0.486	0.391	0.353	0.403	
	60	0.483	0.469	0.369	0.437	
	75	0.481	0.494	0.440	0.473	
Northridge	30	0.436	0.326	0.403	0.384	0.533
	45	0.434	0.336	0.359	0.374	
	60	0.461	0.399	0.338	0.354	
	75	0.480	0.408	0.362	0.377	

Table 10 Maximum base shear of 15-story frames

Record name	Connection capacity (%)	Location patterns for semi rigid connections				Rigid frame (/W)
		Diagonal (/W)	Double diagonal (/W)	Middle (/W)	Middle diagonal (/W)	
Bam	30	0.115	0.091	0.086	0.102	0.141
	45	0.119	0.097	0.092	0.105	
	60	0.123	0.102	0.101	0.107	
	75	0.127	0.107	0.107	0.109	
Chi-Chi	30	0.115	0.104	0.094	0.118	0.134
	45	0.117	0.109	0.103	0.120	
	60	0.120	0.111	0.114	0.090	
	75	0.123	0.112	0.120	0.121	
Imperial	30	0.102	0.097	0.105	0.108	0.121
	45	0.105	0.090	0.101	0.106	
	60	0.107	0.088	0.098	0.101	
	75	0.110	0.095	0.093	0.097	
Kobe	30	0.126	0.090	0.090	0.098	0.150
	45	0.128	0.095	0.091	0.102	
	60	0.131	0.107	0.098	0.109	
	75	0.131	0.118	0.106	0.116	
Northridge	30	0.120	0.102	0.090	0.114	0.134
	45	0.111	0.082	0.091	0.102	
	60	0.114	0.119	0.113	0.124	
	75	0.114	0.123	0.122	0.127	

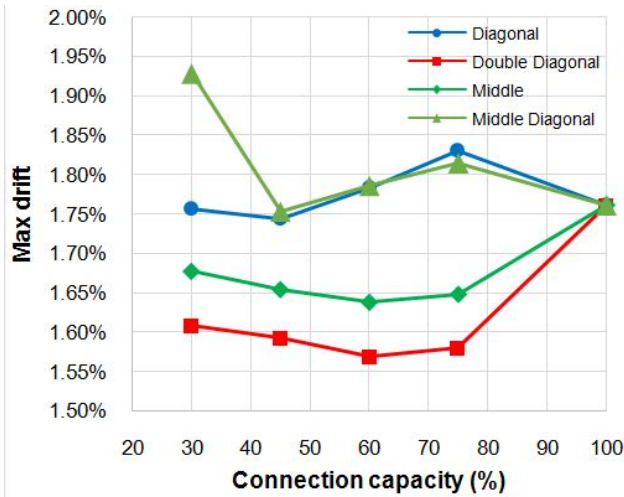


Fig. 31 Maximum story drifts for the 20-story frame

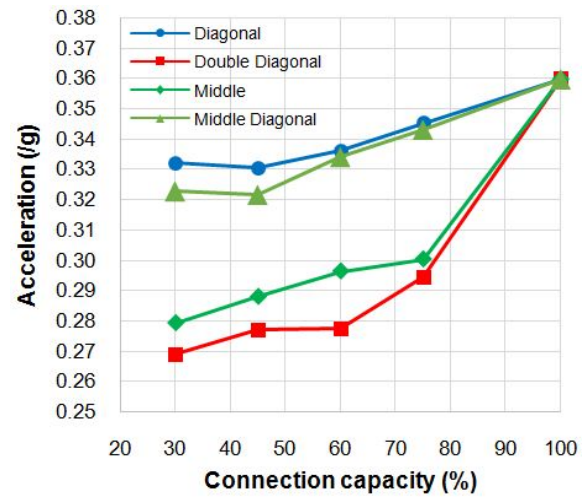


Fig. 32 Maximum roof acceleration for the 20-story frame

Table 11 Maximum story drift of 20-story frames

Record name	Connection capacity (%)	Location patterns for semi rigid connections				Rigid frame (/W)
		Diagonal (%)	Double diagonal (%)	Middle (%)	Middle diagonal (%)	
Bam	30	1.91	1.43	1.54	1.94	1.21
	45	1.73	1.49	1.52	1.97	
	60	1.93	1.42	1.58	2.14	
	75	2.11	1.61	1.53	2.26	
Chi-Chi	30	2.17	1.67	1.72	2.16	2.58
	45	2.25	1.85	1.74	2.14	
	60	2.26	1.88	1.86	2.15	
	75	2.30	1.89	1.94	2.18	
Imperial	30	1.73	1.68	1.72	1.86	1.81
	45	1.99	1.89	1.77	1.91	
	60	1.95	1.89	1.99	1.85	
	75	1.92	1.81	2.03	1.80	
Kobe	30	1.62	1.63	1.77	1.39	1.91
	45	1.43	1.37	1.63	1.48	
	60	1.50	1.33	1.37	1.55	
	75	1.57	1.32	1.37	1.62	
Northridge	30	1.37	1.64	1.69	1.30	1.29
	45	1.31	1.36	1.61	1.27	
	60	1.28	1.32	1.38	1.24	
	75	1.26	1.28	1.36	1.22	

For 20-story frame effect of energy dissipation is more than rigidity decreasing and thus story drifts have decreased. Using semi-rigid connections main period increases and energy dissipating of connections causes the frame to tolerate less base shear and as a result less acceleration. According to Fig. 31, double diagonal pattern has the least maximum story drifts among semi-rigid frames. By choosing the best connection capacity one can reduce maximum story drifts by 1, 11 and 7% in diagonal, double diagonal and middle patterns. Based on Fig. 32, double diagonal pattern has the least maximum roof

acceleration and one can reduce the maximum roof acceleration by 8, 25, 22 and 11% in diagonal, double diagonal, middle and middle diagonal patterns. It can be obtained from Fig. 33 that middle pattern has the least value for maximum base shear and one can reduce this value by 24, 50, 54 and 22% in diagonal, double diagonal, middle and middle diagonal patterns.

Table 14 presents the results comparing seismic performance of the rigid and hybrid frames. Positive number means that value is less in semi-rigid frame while negative number means that value is more in semi-rigid

Table 12 Maximum roof acceleration of 20-story frames

Record name	Connection capacity (%)	Location patterns for semi rigid connections				Rigid frame (/W)
		Diagonal (/g)	Double diagonal (/g)	Middle (/g)	Middle diagonal (/g)	
Bam	30	0.360	0.268	0.285	0.362	0.322
	45	0.359	0.273	0.280	0.350	
	60	0.361	0.270	0.288	0.354	
	75	0.375	0.275	0.278	0.378	
Chi-Chi	30	0.366	0.283	0.295	0.340	0.410
	45	0.357	0.273	0.284	0.329	
	60	0.360	0.272	0.293	0.351	
	75	0.373	0.299	0.318	0.358	
Imperial	30	0.267	0.224	0.237	0.259	0.300
	45	0.281	0.237	0.255	0.261	
	60	0.283	0.236	0.267	0.266	
	75	0.280	0.245	0.274	0.264	
Kobe	30	0.374	0.330	0.341	0.368	0.435
	45	0.377	0.346	0.353	0.374	
	60	0.382	0.350	0.375	0.387	
	75	0.396	0.364	0.356	0.396	
Northridge	30	0.292	0.237	0.238	0.285	0.332
	45	0.278	0.255	0.268	0.294	
	60	0.294	0.258	0.258	0.313	
	75	0.301	0.289	0.276	0.320	

Table 13 Maximum base shear of 20-story frames

Record name	Connection capacity (%)	Location patterns for semi rigid connections				Rigid frame (/W)
		Diagonal (/W)	Double diagonal (/W)	Middle (/W)	Middle diagonal (/W)	
Bam	30	0.077	0.043	0.043	0.079	0.097
	45	0.080	0.054	0.052	0.081	
	60	0.083	0.064	0.063	0.084	
	75	0.086	0.071	0.072	0.086	
Chi-Chi	30	0.075	0.049	0.044	0.073	0.093
	45	0.077	0.057	0.050	0.076	
	60	0.080	0.063	0.057	0.078	
	75	0.082	0.068	0.064	0.079	
Imperial	30	0.059	0.040	0.037	0.063	0.091
	45	0.064	0.047	0.045	0.068	
	60	0.068	0.055	0.051	0.072	
	75	0.071	0.062	0.057	0.077	
Kobe	30	0.074	0.050	0.046	0.073	0.096
	45	0.076	0.056	0.058	0.078	
	60	0.078	0.062	0.063	0.083	
	75	0.083	0.066	0.069	0.086	
Northridge	30	0.061	0.043	0.040	0.065	0.077
	45	0.064	0.047	0.045	0.067	
	60	0.068	0.054	0.053	0.070	
	75	0.071	0.060	0.060	0.071	

Table 14 Maximum response reduction percentages for hybrid frames compared to rigid frames

	Number of stories	Hybrid frames with different location patterns for semi rigid connections			
		Diagonal	Double diagonal	Middle	Middle diagonal
Story drift reduction (%)	10	-5	-7	0	-1
	15	10	11	8	11
	20	1	29	7	0
Roof acceleration reduction (%)	10	13	22	21	12
	15	19	29	25	23
	20	8	25	22	11
Base shear reduction (%)	10	18	32	32	18
	15	15	30	31	32
	20	24	50	54	22

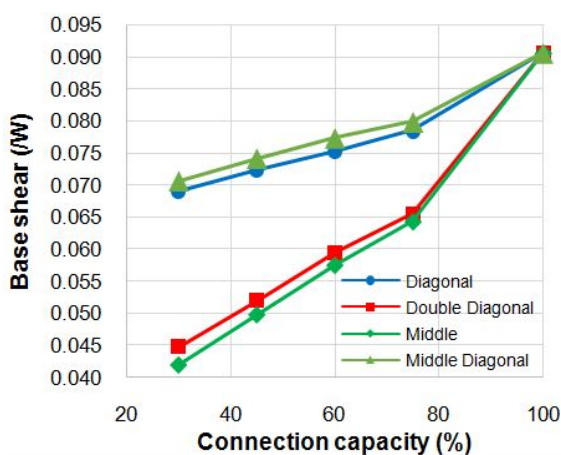


Fig. 33 Maximum base shear for the 20-story frame

frame, i.e., where no improvement has been made using semi-rigid connections.

6. Conclusions

This paper was intended to investigate seismic behavior of semi-rigid steel frame to find out if an improvement occurs compared to rigid frames. For this purpose, 3 rigid frames with 10, 15 and 20 stories were modeled and designed. Using 4 patterns for semi-rigid connection placement patterns and 4 connection capacity percentages, 51 rigid and semi-rigid frames were considered. All frames were subjected to 5 selected earthquake records from which maximum story drifts, roof acceleration and base shear were highlighted.

Numerical analysis results showed that residual displacements in all rigid and semi-rigid are very low. Maximum displacement of roof in semi-rigid frames is less than rigid frame but number of cycles with high maximum displacement in semi-rigid frames is higher. For 10-story frame hysteresis damping in double diagonal and middle pattern is 32 percent higher than other patterns. Semi-rigid connections maximum rotation is equal in all capacities but their maximum moment will increase by increasing connection capacity. One can reduce maximum

roof acceleration of the rigid frames by 22, 29 and 25 percent and base shear by 32, 32 and 54 percent in 10, 15 and 20 story frames with proper semi-rigid connection pattern and capacity. If the main concern is roof acceleration, pattern with more semi-rigid connection including middle and double diagonal pattern should be used. As base shear decreases by using semi-rigid connections one can use smaller sections for beams and columns leading to lighter frames and cost reduction.

References

- Abidelah, A., Bouchaïr, A. and Kerdal, D.E. (2012), "Experimental and analytical behavior of bolted end-plate connections with or without stiffeners", *J. Constr. Steel Res.*, **76**, 13-27.
- AISC 360 (2010), Specification for Structural Steel Buildings, American Institute of Steel Construction; Chicago, IL, USA.
- Akbas, B. and Shen, J. (2003), "Seismic behavior of steel buildings with combined rigid and semi-rigid frames", *Turkish J. Eng. Environ. Sci.*, **27**(4), 253-264.
- ASCE 7 (2010), Minimum Design Loads for Buildings and other Structures, American Society of Civil Engineering; Reston, VA, USA.
- Díaz, C., Victoria, M., Martí, P. and Querin, O.M. (2011), "FE model of beam-to-column extended end-plate joints", *J. Constr. Steel Res.*, **67**(10), 1578-1590.
- Feizi, M.G., Mojtahedi, A. and Nourani, V. (2015), "Effect of semi-rigid connections in improvement of seismic performance of steel moment-resisting frames", *Steel Compos. Struct., Int. J.*, **19**(2), 467-484.
- FEMA 356 (2000), Prestandard and Commentary for the Seismic Rehabilitation of Buildings, Federal Emergency Management Agency; Reston, VA, USA.
- Frye, M.J. and Morris, G.A. (1975), "Analysis of flexibly connected steel frames", *Can. J. Civil Eng.*, **2**(3), 280-291.
- Garlock, M.M., Ricles, J.M. and Sause, R. (2003), "Cyclic load tests and analysis of bolted top-and-seat angle connections", *J. Struct. Eng.*, **129**(12), 1615-1625.
- Ghobarah, A., Osman, A. and Korol, R.M. (1990), "Behavior of extended end-plate connections under cyclic loading", *J. Eng. Struct.*, **12**(1), 15-27.
- Kim, S.E. and Choi, S.H. (2001), "Practical advanced analysis for semi-rigid space frames", *Int. J. Solids Struct.*, **38**(50), 9111-9131.
- Kim, J., Ghaboussi, J. and Elnashai, A.S. (2010), "Mechanical and informational modeling of steel beam-to-column connec-

- tions”, *J. Eng. Struct.*, **32**(2), 449-458.
- Kishi, N., Chen, W.F., Goto, Y. and Hasan, R. (1996), “Behavior of tall buildings with mixed use of rigid and semi-rigid connections”, *J. Comput. Struct.*, **61**(6), 1193-1206.
- Latour, M. and Rizzano, G. (2012), “Experimental behavior and mechanical modeling of dissipative T-stub connections”, *J. Struct. Eng.*, **138**(2), 170-182.
- Mahmoud, H.N., Elnashai, A.S., Spencer Jr., B.F., Kwon, O.S. and Bennier, D.J. (2013), “Hybrid simulation for earthquake response of semirigid partial-strength steel frames”, *J. Struct. Eng.*, **139**(7), 1134-1148.
- Nader, M.N. and Astaneh, A. (1991), “Dynamic behavior of flexible, semi rigid and rigid steel frames”, *J. Constr. Steel Res.*, **18**(3), 179-192.
- Rafiee, A., Talatahari, S. and Hadidi, A. (2013), “Optimum design of steel frames with semi-rigid connections using Big Bang-Big Crunch method”, *Steel Compos. Struct., Int. J.*, **14**(5), 431-451.
- Razavi, M. and Abolmaali, A. (2014), “Earthquake resistance frames with combination of rigid and semi-rigid connections”, *J. Constr. Steel Res.*, **98**, 1-11.
- Sagiroglu, M. and Aydin, A.C. (2015), “Design and analysis of non-linear space frames with semi-rigid connections”, *Steel Compos. Struct., Int. J.*, **18**(6), 1405-1421.
- Shi, G., Shi, Y. and Wang, Y. (2007), “Behavior of end-plate moment connections under earthquake loading”, *J. Eng. Struct.*, **29**(5), 703-716.
- Stelmack, T.W., Marley, M.J. and Gerstle, K.H. (1986), “Analysis and tests of flexibly connected steel frames”, *J. Struct. Eng.*, **112**(7), 1573-1588